CONCLUSION

The present kinetic study revealed faster initial myocardial uptake and liver clearance of tetrofosmin in comparison to MIBI. This leads to a favorable time window for image acquisition with tetrofosmin between 30 and 60 min after tracer injection. However, the faster clearance may represent a disadvantage for delayed myocardial imaging, since the tracer distribution may not only reflect blood flow. Future experimental and clinical studies are required to define the tetrofosmin kinetics in ischemic myocardium in order to exclude the possibility of redistribution by differential washout in normal and ischemic myocardium.

ACKNOWLEDGMENTS

We thank Anneliese Aigner, Winfried Bachmann, Gitti Dzewas, Monika Krapf and Gernot Leitner for excellent technical assistance. Andreas Sailer for reliable quality control of the camera and Dr. Günther Reidel for radiochemical purity testing.

REFERENCES

1. Zaret BL, Wackers FJ. Nuclear cardiology. *N Engl J Med* 1993;329:775–783.
2. Zaret BL, Wackers FJ. Nuclear cardiology. *N Engl J Med* 1993;329:855–863.
3. Beller GA. Myocardial perfusion imaging with thallium-201. *J Nucl Med* 1994;35: 674–680.
4. Nakajima K, Taki J, Bunko H, et al. Dynamic acquisition with a three-headed SPECT system: application to technetium-99m-SQ30217 myocardial imaging. *J Nucl Med* 1991;32:1273–1277.
5. Leppo JA, DePuey EG, Johnson LL. A review of cardiac imaging with sestamibi and teboroxime. *J Nucl Med* 1991;32:2021–2022.
6. Wackers FJT, Berman DS, Maddahi J, et al. Technetium-99m hexakis 2-methoxyisobutyl isonitrile: human biodistribution, dosimetry, safety and preliminary comparison to thallium-201 for myocardial perfusion imaging. *J Nucl Med* 1989;30:301–311.
7. Kelly JD, Forster AM, Higley B, et al. Technetium-99m-tetrofosmin as a new radiopharmaceutical for myocardial perfusion imaging. *J Nucl Med* 1993;34:222–227.
8. Higley B, Smith FW, Smith T, et al. Technetium-99m-1,2-bis[bis(2-ethoxyethyl) phosphino]ethane: human biodistribution, dosimetry and safety of a new myocardial perfusion imaging agent. *J Nucl Med* 1993;34:30–38.
9. Nakajima K, Taki J, Shuke N, Bunko H, Takata S, Hisada K. Myocardial perfusion imaging and dynamic analysis with technetium-99m-tetrofosmin *J Nucl Med* 1993; 34:1478–1484.
10. Jain D, Wackers FJ, Mattera J, McMahon M, Sinusas AJ, Zaret BL. Biokinetics of technetium-99m-tetrofosmin: myocardial perfusion imaging agent: implications for a one-day imaging protocol. *J Nucl Med* 1993;34:1254–1259.
11. Sinusas AJ, Shi Q, Saltzberg MT, et al. Technetium-99m-tetrofosmin to assess myocardial blood flow: experimental validation in an intact canine model of ischemia. *J Nucl Med* 1994;35:664–671.
12. Rigo P, Leclercq B, Itti R, Lahiri A, Braat S. Technetium-99m-tetrofosmin myocardial imaging: a comparison with thallium-201 and angiography. *J Nucl Med* 1994;35:587–593.
13. Zaret BL, Rigo P, Wackers FJ, et al. Myocardial perfusion imaging with ^{99m}Tc tetrofosmin. Comparison to ^{201}Tl imaging and coronary angiography in a Phase III multicenter trial. Tetrofosmin International Trial Study Group. *Circulation* 1995;91: 313–319.
14. Tamaki N, Takahashi N, Kawamoto M, et al. Myocardial tomography using technetium-99m-tetrofosmin to evaluate coronary artery disease. *J Nucl Med* 1994;35:594–600.
15. Flamen P, Bossuyt A, Franken PR. Technetium-99m-tetrofosmin in dipyridamol-stress myocardial SPECT imaging: intraindividual comparison with technetium-99m-sestamibi. *J Nucl Med* 1995;36:2009–2015.
16. Piwnica-Worms D, Kronauge JF, Chiu ML. Uptake and retention of hexakis (2-methoxyisobutyl isonitrile) technetium (I) in cultured chick myocardial cells. Mitochondrial and plasma membrane potential dependence. *Circulation* 1990;82:1826–1838.
17. Platts EA, North TL, Pickett RD, Kelly JD. Mechanism of uptake of technetium-99m-tetrofosmin. I. uptake into isolated adult rat ventricular myocytes and subcelluar localization. *J Nucl Cardiol* 1995;2:317–326.
18. Younes A, Songadele JA, Maublant J, Platts E, Pickett R, Veyre A. Mechanism of uptake of technetium-99m-tetrofosmin. II. Uptake into isolated adult rat heart mitochondria. *J Nucl Cardiol* 1995;2:327–333.
19. Piwinca-Worms D, Kronauge JF, Holmann BL, Davison A, Jones AG. Comparative myocardial uptake characteristics of hexakis (alkylisonitrile)technetium(I) complexes: effect of lipophilicity. *Invest Radiol* 1989;24:25–29.
20. Wolfe CL, O'Connell JW, Sievers RE, Cobb C, Dae MW, Botvinick E. Assessment of perfused left ventricular mass in normal, ischemic and reperfused myocardium by means of SPECT of technetium-99m isonitrile. *Am Heart J* 1993;126:1275–1286.
21. Glover DK, Okada RD. Myocardial kinetics of ^{99m}Tc-MIBI in canine myocardium after dipyridamole. *Circulation* 1990;81:628–637.
22. Taillefer R, Laflamme L, Dupras G, Picard M, Phaneuf DC, Leveille J. Myocardial perfusion imaging with ^{99m}Tc-MIBI: comparison of short and long time intervals between rest and stress injections. *Eur J Nucl Med* 1988;13:515–522.

Myocardial Perfusion and Function Imaging at Rest with Simultaneous Thallium-201 and Technetium-99m Blood-Pool Dual-Isotope Gated SPECT

André Constantinesco, Luc Mertz and Bernard Brunot

Departments of Nuclear Medicine and Biophysics, CHU Hautepierre, Strasbourg, France

We present a simultaneous gated SPECT (G-SPECT) dual-isotope technique using ^{201}Tl for perfusion and ^{99m}Tc blood-pool labeling for function imaging. **Methods:** Seventeen patients (13 with previous myocardial infarction, MI) and a control group of three normal volunteers were investigated. They received, 15 min after a ^{201}Tl stress/redistribution protocol with reinjection, 900–950 MBq ^{99m}Tc-HSA for blood-pool labeling. Eight frames per R-R interval were recorded in the G-SPECT mode with three windows: window A with 20% centered at 71 keV for ^{201}Tl, window B with 10% centered at 105 keV for Tc scatter contamination and window C centered at 140 keV with 20% for ^{99m}Tc. Nongated, crosstalk-corrected ^{201}Tl SPECT perfusion images were reconstructed according to normalized projection-by-projection subtraction from data from windows A and B. G-SPECT data from window C were reconstructed with the same reconstruction limits to allow topographic correlations of left ventricular perfusion and wall motion abnormalities. Polar maps of perfusion and function were used to divide the myocardium into 20 segments. Perfusion was expressed as the percentage of thallium uptake and function corresponding to diastolic to systolic shortening normalized by end diastolic volume. **Results:** Segmental comparison of uncontaminated-to-contaminated and corrected ^{201}Tl patient images demonstrated an overall agreement score of 93%, with a kappa statistic of 0.76 ± 0.06 when normal perfused segments were excluded. Segmental matching of perfusion against function at rest showed no correlation for the 10 patients with preserved ejection fraction of 59% ± 8% nor for the control group. For the remaining seven patients with an ejection fraction of 34% ± 10%, there was linear correlation between perfusion and function (r^2 = 0.61). **Conclusions:** The feasibility of dual Tl-Tc G-SPECT was examined at rest and suggests low perfusion hypokinesis that matches linear dependence for CAD patients with low ejection fraction.

Key Words: myocardial perfusion; dual-isotope imaging; thallium-201; technetium-99m; gated SPECT; left ventricular function

J Nucl Med 1997; 38:432–437

Received Feb. 2, 1996; revision accepted Jul. 15, 1996.

For correspondence or reprints contact: Andre Constantinesco, MD, PhD, Departments of Nuclear Medicine and Biophysics, CHU Hautepierre, 1 Av. Moliere, Strasbourg 67098 France.

Nuclear imaging of left ventricular myocardial perfusion and function at rest ideally requires simultaneous acquisition of both parameters (*1*). For simultaneous routine assessment of myocardial perfusion and function, some authors have developed a gated SPECT (G-SPECT) technique using ^{99m}Tc-sestamibi, which determines myocardial function at rest by measuring systolic/diastolic changes in wall thickening (*2–4*). This interesting technique, which is based on the use of only one isotope, needs clinical validation because it appears fairly difficult to accurately determine wall thickening modifications in severely hypoperfused areas with a flow agent. To overcome this limitation, we propose a simultaneous dual-isotope G-SPECT technique using ^{201}Tl for perfusion and ^{99m}Tc labeled blood pool for function imaging. Simultaneous dual-isotope SPECT techniques with two windows (centered on photopeaks) combining perfusion/viability agents such as ^{201}Tl and ^{99m}Tc-sestamibi show an important contribution of ^{99m}Tc crosstalk in the ^{201}Tl window, but only a very low level of ^{201}Tl crosstalk in the ^{99m}Tc window (*5–7*). These studies demonstrated the need to correct for ^{99m}Tc crosstalk in the ^{201}Tl window because the use of only two windows for simultaneous ^{201}Tl/^{99m}Tc dual-isotope acquisition leads to large systematic underestimation of the ^{201}Tl defect severity score. However, acquisition techniques with three or four windows using simultaneous ^{201}Tl/^{99m}Tc dual-isotope SPECT acquisition permits the use of various methods to significantly reduce spilldown scatter contamination of ^{99m}Tc into the ^{201}Tl window, giving good results in patients and phantom studies (*8–13*). In an earlier phantom and patient study, we validated a three-window dual-isotope G-SPECT acquisition method using ^{201}Tl for perfusion and ^{99m}Tc labeled blood pool for function, with a spilldown correction based on a simple window subtraction technique (*14*).

The aim of this study was to explore the feasibility of three-window dual-isotope G-SPECT acquisition using ^{201}Tl for perfusion and ^{99m}Tc blood pool for function, with a spilldown correction method based on a Monte Carlo simulation model proposed by Weinstein et al. (*9*) and Hademenos et al. (*10,11*) and to demonstrate the utility of simultaneous imaging of perfusion and function for topographic correlation in normal and hypoperfused myocardial areas of 17 patients.

MATERIALS AND METHODS

Patients

The study population consisted of 17 consecutive patients (14 men, 3 women; mean age 63.7 yr) who were referred for stress/redistribution (with reinjection) myocardial scintigraphy for coronary artery disease evaluation (n = 4) or residual chest pain after myocardial infarcton (MI) (n = 13). The patients were divided into two groups according to the normal limits of ejection fraction used in our department (*15*): Group 1 (10 patients) with a preserved resting ejection fraction of 59% ± 8% and Group 2 (7 patients) with a low resting ejection fraction of 34% ± 10%. In addition, three normal volunteers with an ejection fraction of 61% ± 2% were used as controls (Table 1).

Perfusion and Function Tracers

The general protocol used in this study, described in Figure 1, permits comparison of uncontaminated compared with contaminated and corrected ^{201}Tl images and also allows correlations of perfusion and function at rest. The first part of the protocol consisted of a ^{201}Tl SPECT stress [exercise in five patients or dipyridamole (0.56 mmg/kg for 4 min in 12 patients)] and ^{201}Tl redistribution with reinjection 4 hr later. This procedure was then followed, in a second part, 15 min later, by blood pool labeling with ^{99m}Tc-human serum albumin (HSA) before the dual G-SPECT acquisition. Finally a resting standard planar LAO projection left ventricular ejection fraction was also obtained. We used ^{201}Tl (111–130 MBq) for perfusion and ^{99m}Tc-HSA blood pool labeling (900–950 MBq) for function, taking into account patient weight.

TABLE 1
Patient Data

Patient no.	Age (yr)	Sex	MI/CAD	Coronarography	LVEF (%)	DIP/Ex	Delay MI/Scint.	EDV (ml)
1	69	M	Inf	RCA 100% Cx 100%	52	DIP	10 mo	189
2	72	F	Inf	RCA 90%	56	DIP	1 yr	37
3	69	F	Post/Inf	Cx 95%	75	DIP	5 yr	89
4	75	M	Inf	RCA 90%	57	DIP	1 mo	155
5	53	F	CAD	3 vessels BG	71	Ex	2 yr	86
6	43	M	Ant/Lat	LDA 70%	51	Ex	10 mo	121
7	81	M	CAD	/	61	DIP		109
8	62	M	CAD	Cx PTCA	57	DIP	2 yr	65
9	58	M	Inf	RCA 100% LDA 60%	55	DIP	2 yr	132
10	70	M	CAD	/	55	Ex		110
11	52	M	Ant	LDA 80% Cx 70%	27	Ex	1.5 yr	141
12	69	M	Ant/ Sept	LDA 35% Cx 90%	50	DIP	2 mo	151
13	70	M	Ant	LDA 90% Cx 70%	32	DIP	1 yr, 3 mo	169
14	75	M	Ant/Inf	LDA 80% Cx 80%	15	DIP	1 yr, 2 mo	188
15	49	M	Ant	LDA 90%	43	Ex	11 mo	149
16	67	M	Ant/ Sept	LDA 95%	44	DIP	1 mo, 15 days	160
17	50	M	Ap/Inf	LDA 100% RCA 100%	33	DIP	1 yr	190
18	30	M			63	Rest		145
19	26	M			61	Rest		162
20	50	M			58	Rest		137

MI = myocardial infarction; Inf = inferior; Ant = anterior; Ap = apical; Sept = septal, post = posterior; Lat = lateral; CAD = coronary artery disease evaluation; coronarography = % of vessel stenosis; RCA = right coronary artery; Cx = circumflex artery; LDA = left descending artery; PTCA = angioplasty; BG = bypass graft; LVEF = rest left ventricular ejection fraction; DIP = dyridamole; Ex = exercise; EDV = end diastolic volume. Group 1 patients (nos. 1–10); Group 2 (Patients 11–17).

SPECT Imaging

For the first part of the protocol, standard ^{201}Tl stress (exercise or dipyridamole)/redistribution with reinjection 4 hr later, we used a rectangular camera equipped with a low-energy, high-resolution collimator (30 projections of 40 sec, 180° arc rotation and body contour from the 45° right anterior oblique position to the left posterior oblique position, patients were in supine position). A window with 20% centered at 71 keV for ^{201}Tl was used. Each projection image was corrected for uniformity and center of rotation correction was also performed. Thallium-201 SPECT images were reconstructed with filtered backprojection using a Butterworth filter with a cutoff frequency of 0.35. Reconstructions

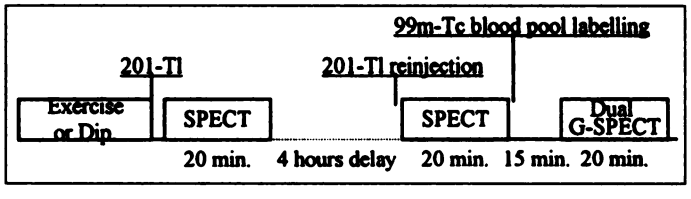

FIGURE 1. Schematic outline of the protocol used in this study.

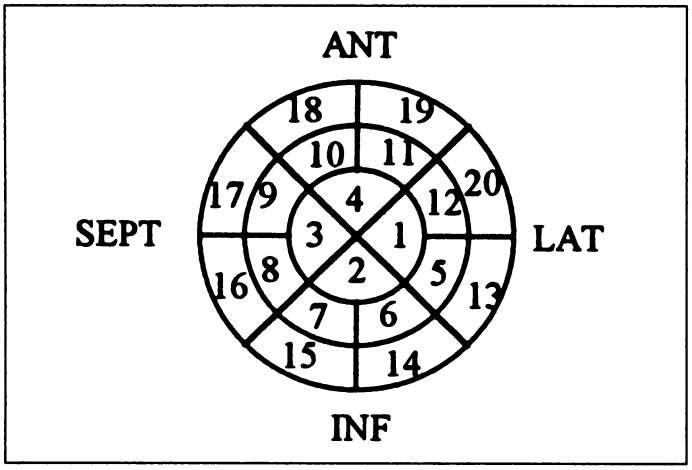

FIGURE 2. Topographic representation of the 20 segments determined on the polar maps (perfusion and function). ANT = anterior; SEPT= septum; INF = inferior; LAT = lateral.

produced tomograms of 12-mm axial slices encompassing the heart.

Dual G-SPECT Acquisition and Processing

For the second part of the protocol, we used the same low-energy, high-resolution collimator. A three-window acquisition method was used to significantly reduce the crosstalk between ^{99m}Tc and ^{201}Tl: window A with 20% centered at 71 keV for ^{201}Tl, window B centered at 105 keV with 10% for Tc scatter and window C centered at 140 keV with 20% for ^{99m}Tc. Eight frames per R-R interval were recorded in the G-SPECT mode for the three windows (30 projections of 40 sec, 64 × 64 images, 180° arc rotation and body contour from the 45° right anterior oblique position to the left posterior oblique position). Each projection image was corrected for uniformity and center of rotation. Total acquisition time was 20 min.

Nongated ^{201}Tl and ^{99m}Tc scatter images were then obtained by adding the 8 frames of each projection of windows A and B. After nine-point spatial smoothing of the summed frames from windows A and B, crosstalk correction from ^{99m}Tc scatter into the ^{201}Tl window was performed by subtracting projection-by-projection the previous summed frames of windows A and B using weighted coefficients based on the Monte Carlo simulation model proposed by Hademenos et al. (*10,11*). Crosstalk-corrected ^{201}Tl SPECT images were then reconstructed using filtered backprojection. The same limits, reorientation angles and slice thicknesses as those used for reconstruction of crosstalk-corrected ^{201}Tl SPECT images were then applied to the reconstruction of blood-pool G-SPECT images using data from the ^{99m}Tc window (window C). This procedure ensured that the perfusion slices corresponded topographically to the function slices. Both reconstructions (corrected ^{201}Tl and ^{99m}Tc blood pool) produced homologous corresponding tomograms of 12-mm axial slices encompassing the entire heart. In addition, after the dual G-SPECT procedure, we measured left ventricular ejection fraction for each patient in planar mode using an LAO projection with 32 images per cardiac cycle.

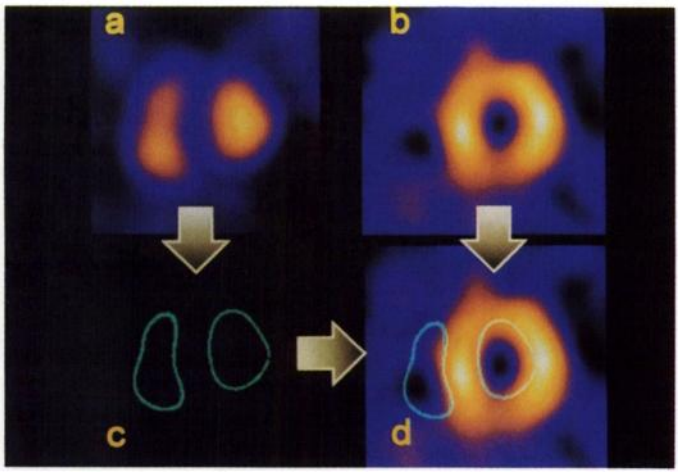

FIGURE 3. Corresponding slices of (A): end-diastolic ^{99m}Tc blood-pool and (B) nongated ^{201}Tl dual short-axis images. (C) 45% threshold end-diastolic isocontour of image (A). (D) Superposition of both (C) and (B) images.

TABLE 2
Segmental Agreement between Dual and Virgin Rest ^{201}Tl Images for Groups 1 and 2

	Virgin ^{201}Tl			
Score	0	1	2	3
Dual ^{201}Tl				
0	111	20	0	0
1	12	156	7	0
2	0	7	26	0
3	0	0	0	1

Exact agreement: 90%, $\kappa = 0.80 \pm 0.03$.

Image Analysis

For the purpose of this study, redistribution-reinjection ^{201}Tl SPECT images acquired before the dual procedure, and therefore uncontaminated by ^{99m}Tc crosstalk, are denoted virgin ^{201}Tl images. The ^{201}Tl images extracted from the simultaneous three windows dual-isotope procedure described above are denoted dual ^{201}Tl images.

Virgin and Dual Rest Thallium-201 Tomograms

Maximum counts normalized bull's-eyes polar maps of virgin and dual rest ^{201}Tl tomograms were constructed using apical, mid and basal cuts of short-axis slices plus the midvertical long and horizontal axis slices. The ^{201}Tl myocardial perfusion bull's-eyes were then divided into 20 segments for each patient. These segments were defined as regions representative of the anterior, septal, inferior, lateral and apical walls (Fig. 2). To overcome obvious limitations of visual scoring of perfusion defects, relative isotope uptake of each segment was scored by an automated algorithm using a linear four-level scale (from 0 to 3), in which relative isotope uptake corresponded respectively to 76%–100%, 51%–75%, 26%–50%, and 0%–25% of the maximum of the bull's-eye image.

Gated Blood-Pool Tomograms at Rest

Left ventricular isocontours were determined for each of the eight frames/R-R cycle by an automated algorithm using a 45% threshold of the left ventricular maximum counts of the whole dataset of blood-pool tomograms, with the base or mitral valve plane determined using the "0" stroke volume method (*16*). The 45% threshold corresponding to the best contour determination was demonstrated in phantoms in a previous study (*14*). The tomograms of both nongated thallium and technetium blood-pool images were calculated with the same limits, angles and slice thicknesses. The left ventricular blood-pool endocardial isocontours or "function slices" could therefore be superposed over corresponding "perfusion slices" obtained from nongated dual ^{201}Tl images to simultaneously display myocardial perfusion/function images in both static or cine mode (Fig. 3).

Left ventricular function at rest was also analyzed and quantified using horizontal short- and vertical long-axis ^{99m}Tc blood-pool G-SPECT images by construction of a bull's-eye polar map expressing wall motion by diastolic-to-systolic radial shortening of endocardial contours. We used a hybrid method with a floating

TABLE 3
Mean, Minimal (Min.), Maximal (Max.) and Standard Deviation (s.d.) Values of Perfusion and Function for Control Subjects and Group 1 and 2 Patients

	Control (n = 60)		Group 1 (n = 200)		Group 2 (n = 140)	
	Perfusion (%)	Function (mm^{-2})	Perfusion (%)	Function (mm^{-2})	Perfusion (%)	Function (mm^{-2})
Mean	74	8.5	73*	7.5*	63†	2.5†
s.d.	7	3	9	5	15	3
Min.	59	0.5	45	−3	20	−7
Max.	88	14.5	90	26	89	9

*Nonsignificant versus control.
†$p < 0.0001$ versus Group 1 and control.
Minus sign indicates paradoxical motion. Group 1 had a mean ejection fraction of 59% ± 8%. Group 2 had a mean ejection fraction of 34% ± 10%. Control group had a mean ejection fraction of 61% ± 2%. n = the number of segments.

frame for mid and basal short-axis slices and a fixed frame for the apex and vertical long-axis slices (*16*). With the same topographic segmentation (20 segments) used for the perfusion study, we defined a normalized segmental wall motion index by dividing the segmental diastolic-to-systolic radial shortening by the end diastolic volume for each patient (*18*). This normalized function bull's-eye polar map was then compared to the corresponding perfusion bull's eye-polar map obtained simultaneously for regional correlation of perfusion and function.

Statistical Analysis

For analysis of segmental agreement between virgin and dual rest ^{201}Tl images, the kappa (k) statistic and its s.e. were used as a measure of agreement. A value of 1 denotes perfect agreement, while 0 indicates no agreement beyond chance. It is admitted that k values ≧ 0.6 correspond to a good agreement. For analysis of segmental perfusion-function matching we used linear regression relationships. One factor variance analysis was used to assess differences of perfusion or function among groups. A p value < 0.05 was considered significant.

RESULTS

Comparison of Virgin and Dual Rest Thallium-201 Images

Segmental Score Agreement of Virgin and Dual Rest Thallium-201 Images. Table 2 shows the segmental score agreement between virgin and dual ^{201}Tl images for Group 1 and 2 patients. Control group results were not considered for this comparison because they would artificially improve the kappa value. For the 340 segments, the overall agreement score was 90%, with a kappa statistic of 0.80 ± 0.03 When the segments with a visual score of 0 were excluded, the agreement between dual and virgin images was 93%, with a kappa statistic of 0.76 ± 0.06.

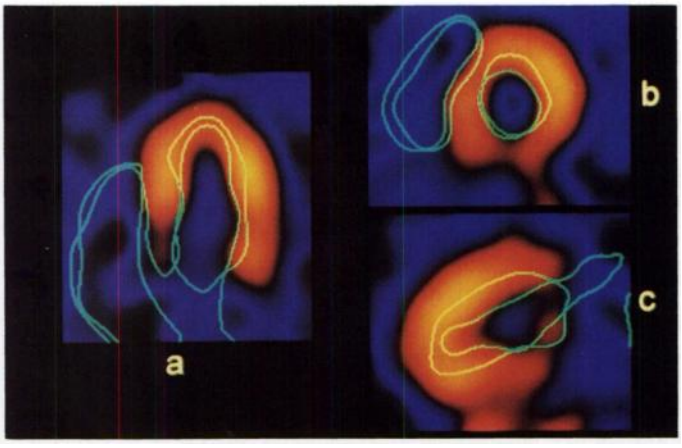

FIGURE 4. Patient 4 with an ejection fraction of 57%. Selected midventricular dual ^{201}Tl images and corresponding systolic and diastolic contours show normal septo-apical perfusion but corresponding hypokinetic wall motion (A,B) and a posterobasal perfusion defect (MI scar) with akinetic wall motion (C).

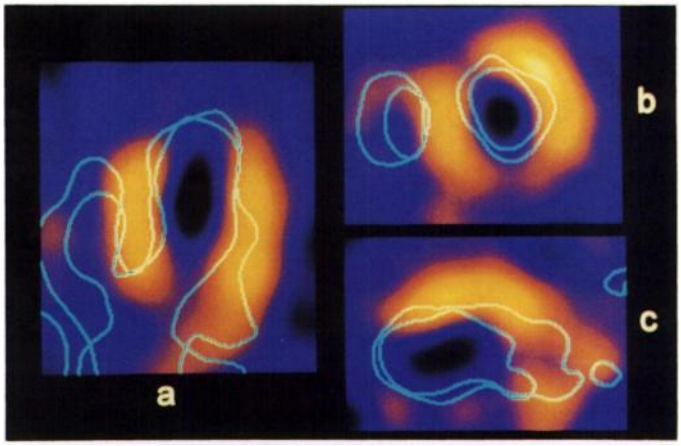

FIGURE 5. Patient 17 with ejection fraction of 33%. Selected midventricular dual ^{201}Tl images and corresponding systolic and diastolic contours show extended apical and inferior perfusion defects associated with dyskinetic, hypokinetic and akinetic wall motion abnormalities (A,C). A small anterior wall perfusion defect demonstrates normal contraction (B).

Perfusion and Function Analysis

Segmental Perfusion and Function Quantitation. Segmental perfusion of patients and control subjects, expressed as percent relative thallium uptake, varied between 20% and 90%, while the corresponding function index, expressed as the normalized wall motion index (by dividing the segmental systolic-to-diastolic endocardial motion by the end-diastolic volume), varied between −7 [mm^{-2}] and +26 [mm^{-2}] (Table 3). No significant differences were found for the relative thallium uptake and function index between Group 1 patients and the

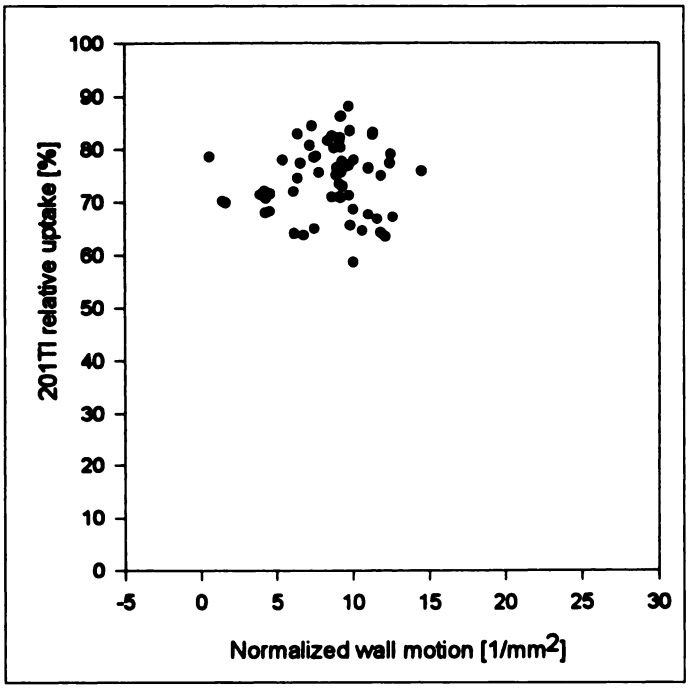

FIGURE 6. Rest segmental perfusion and function correlation from dual G-SPECT acquisition and for group control with normal ejection fraction of 62% ± 3%. Linear regression coefficient is $r^2 = 0.01$

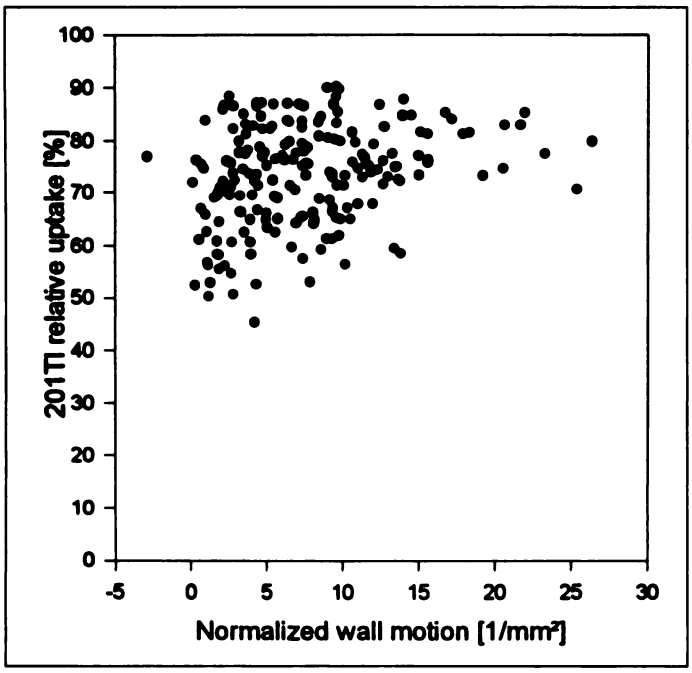

FIGURE 7. Rest segmental perfusion and function correlation from dual G-SPECT acquisition and for Group 1 patients with normal ejection fraction of 59% ± 8%. Linear regression coefficient is $r^2 = 0.01$

control group, but the relative thallium uptake and function index were significantly lower in Group 2 patients compared with Group 1 and the control group ($p < 0.0001$) (Table 3).

Resting Perfusion-Function Correlations

Patient 4. This 75-yr-old man was referred 1 mo after an inferior MI because he had residual chest pain. Coronarography showed 90% stenosis of the RCA and LVEF was subnormal at 57% (normal limits in our department are 62% ± 3%). On selected midventricular dual ^{201}Tl images (Fig. 4), there is only an inferior and basal fixed defect corresponding to the MI. The

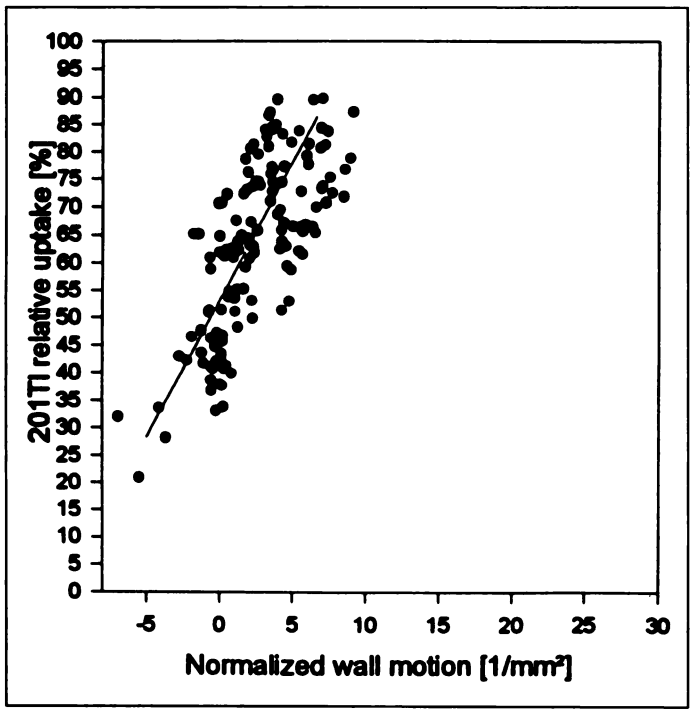

FIGURE 8. Rest segmental perfusion and function correlation from dual G-SPECT acquisition and for Group 2 patients with low ejection fraction of 34% ± 10%. Linear regression coefficient is $r^2 = 0.61$

superimposed homologous function images represented by diastolic and systolic contours show decreased motion of the septo-apical wall, demonstrating normal perfusion but hypokinetic myocardium and a localized akinetic area corresponding to the MI scar.

Patient 17. This 50-yr-old man was referred 1 yr post-MI. Coronarography showed occlusion of the LDA and circumflex arteries and his LVEF was 33%. Figure 5 shows a selected set of short, vertical long and horizontal long-axis midventricular slices of dual ^{201}Tl images associated with systolic and diastolic contours obtained simultaneously. This dataset, which allows direct visual assessment of regional wall motion abnormalities and the corresponding perfusion, demonstrates extended and severe apical and inferior perfusion defects corresponding to dyskinetic, hypokinetic and akinetic wall motion areas but also a moderate perfusion defect in the anterior wall with normal contraction.

Segmental Topographic Relationships between Perfusion and Function at Rest

Figures 6 and 7 show the lack of topographic perfusion-function linear correlations between thallium uptake and normalized wall motion index for the control group and for Group 1 patients who had preserved ejection fraction (59% ± 8%). In contrast, we found a linear correlation ($r^2 = 0.61$) between the relative thallium uptake and the normalized wall motion index for Group 2 patients who had a low ejection fraction (34% ± 10%) (Fig. 8).

DISCUSSION

In ^{201}Tl/^{99m}Tc imaging, there is significant crosstalk of ^{99m}Tc photons in the thallium window due to their higher energy, but the ^{201}Tl crosstalk into the ^{99m}Tc energy window is low (about 2.9% ± 2.1% of the registered Tc counts). This was not considered in our study (*5*). The crosstalk of ^{99m}Tc photons in the ^{201}Tl window was shown to contribute 27% of the dual ^{201}Tl counts, with a 22% reduction in normalized defect severity between virgin and dual ^{201}Tl (*6*). To reduce this crosstalk, a three-window technique with projection-by-projection subtraction correction based on a Monte Carlo attenuation simulation model proposed by Weinstein et al. (*9*) and Hademenos et al. (*10,11*) was applied to the dual thallium-technetium G-SPECT acquisition.

The present data show that this spilldown correction method enhances the agreement score between dual and virgin ^{201}Tl images. The agreement score, determined by measuring the percent thallium uptake, was higher in our study ($k = 0.80$) compared to the value of $k = 0.51$ obtained by Kiat et al. (*6*). Several other spilldown correction methods are now available for dual-isotope imaging. However, we could not use the correction method proposed by Moore et al. (*12*) because the gamma camera could not simultaneously acquire four windows in a gated mode with more than four frames per cardiac cycle. Even with three simultaneous windows, as in the protocol we used, our system was limited to eight frames per cardiac cycle. This results in uncertainty in the determination of the blood-pool end-systolic image, leading to underestimation of radial diastolic/systolic shortening. Another recently proposed compensation method for correction of ^{99m}Tc spilldown in the ^{201}Tl window using convolution of two windows centered on thallium and technetium photopeaks could overcome this problem (*13*). The methods for detecting viable myocardium depend on the assessment of myocardial metabolism, cellular membrane integrity and wall motion, but it is clinically recognized that the ultimate aim is to detect patients capable of wall motion

recovery after revascularization (*19*). Laboratory and clinical investigations have suggested that matching between low perfusion and reduced myocardial contractile function in acute short-term ischemia (stunned myocardium) is dominated by the reduction of subendocardial blood flow and that sustained or chronic ischemia (hibernating myocardium) may be related to compensatory processes that permit improvement of wall motion after revascularization (*20*). However, low perfusion hypokinesis function matching needs to be observed simultaneously knowing that wall motionn can also develop as perfusion abnormalities (*21*) and that hypofixation of the inferior wall may be partially related to attenuation.

These data illustrate the clinical interest of simultaneously recording myocardial perfusion and function essentially in low and very low perfused segments. In our preliminary series of normal individuals and patients at rest, we confirmed that there is no correlation with wall motion when segmentary myocardial perfusion (expressed by relative thallium uptake) is normal or slightly reduced. This could be explained by the fact that normal perfused regions can have a variable range of motion, for example, septal wall expansion, which is less than that of the lateral wall (*16,18*). However, when myocardial perfusion is greatly reduced, we found a segmental perfusion-function linear relationship. This low perfusion hypokinesis matching, which needs confirmation in a larger population of patients, was first observed in laboratory animals in ischemic experimental protocols (*20*). Recently, significant correlation was also found between the quantitative systolic wall thickening index and the corresponding thallium defect visual scores using a planar stress/reinjection ^{201}Tl protocol and delayed rest, planar gated ^{99m}Tc-sestamibi (*22*).

CONCLUSION

If myocardial perfusion and function could be acquired simultaneously, many sources of topographic errors or motion artifacts associated with separate acquisition protocols would be eliminated. The three-window dual-isotope gated SPECT method used in this study has the potential to enhance the quality of thallium images contaminated by technetium cross-talk, thereby permitting simultaneous myocardial perfusion/function topographic analysis at rest. Furthermore, the analysis of wall motion becomes independent of wall perfusion, which is in contrast to the resting G-SPECT sestamibi protocol (*4*). Although our method cannot be applied in stress tests such as exercise or dipyridamole, we have recently proposed a resting/low-dose dobutamine dual thallium-technetium G-SPECT protocol that should be capable of differentiating reversible from fixed wall dysfunction of hypoperfused myocardial areas (*23*).

ACKNOWLEDGMENTS

This study was supported by a grant CFR95051 from CIS BIO International.

REFERENCES

1. Borges-Neto S, Coleman R, Jones R. Perfusion and function at rest and treadmill exercise using Tc-99m-sestamibi: comparison of one- and two-day protocols in normal volunteers. *J Nucl Med* 1990;31:1128–1132.
2. Mercassa G, Marzullo P, Pandi O, Sambuceti G, L'Abbate A. A new method for noninvasive quantitation of segmental myocardial thickening using ^{99m}Tc-sestamibi: results in normal subjects. *J Nucl Med* 1990;31:173–177.
3. Faber T, Akers M, Peschock R, Corbett J. Three-dimensional motion and perfusion quantification in gated single-photon emission computed tomograms. *J Nucl Med* 1991;32:2311–2317.
4. Germano G, Kiat H, Kavanagh P, et al. Automatic quantification of ejection fraction from gated myocardial perfusion SPECT. *J Nucl Med* 1995;36:2138–2147.
5. Kiat H, Germano G, Van Train K, et al Quantitative assessment of photon spillover in simultaneous rest ^{201}Tl/stress ^{99m}Tc-sestamibi dual-isotope myocardial perfusion SPECT.[Abstract]. *J Nucl Med* 1992;33(suppl):854P.
6. Kiat H, Germano G, Friedman J, et al. Comparative feasability of separate or simultaneous rest thallium-201 stress technetium-99m-sestamibi dual-isotope myocardial perfusion SPECT. *J Nucl Med* 1994;35:542–548.
7. Lowe V, Greer K, Hanson M, Jaszczak R, Coleman R. Cardiac phantom evaluation of simultaneously acquired dual-isotope rest thallium-201/stress technetium- 99m SPECT imaging. *J Nucl Med* 1993;34:1998–2005.
8. Yang DC, Ragasa E, Gould L, et al. Radionuclide simultaneous dual-isotope stress myocardial perfusion study using the three-window technique. *Clin Nucl Med* 1993;18:852–857.
9. Weinstein H, Hademenos G, Rheinhardt C, McSherry B, Wironnen J, Leppo J. A new method of simultaneous dual-isotope ^{99m}Tc/^{201}Tl imaging and spilldown correction [Abstract]. *Circulation* 1992;86:I-707.
10. Hademenos G, Ljungberg M, King M A, Glick S J. A Monte Carlo investigation of the dual photopeak window scatter correction method. *IEEE Trans Nucl Sci* 1993;40:179–185.
11. Hademenos G, Dahlbom M, Hoffman E. Simultaneous dual-isotope technetium-99m/thallium-201 cardiac SPET imaging using a projection-dependent spilldown correction factor. *Eur J Nucl Med* 1995;22:465–472.
12. Moore SC, Syravanh C, Tow DE. Simultaneous SPET imaging of ^{201}Tl and ^{99m}Tc using four energy windows [Abstract]. *J Nucl Med* 1993;34(suppl):188P.
13. Knesaurek K. A new dual-isotope convolution cross-talk correction method: a ^{201}Tl/^{99m}Tc SPECT cardiac phantom study. *Med Phys* 1994;21:1577–1583.
14. Constantinesco A, Mertz L, Brunot B, Ravier S, Choquet P. A new thallium-technetium dual-isotope G-SPECT technique for simultaneous myocardial perfusion and motion analysis. *Med Nucl* 1995;19:190–198.
15. Richard P, Mossard J, Constantinesco A, et al. Validity of total ejection fractions according to the presence or the absence of left ventricular dyskinesias: comparison between contrast angiography and angioscintigraphy. *Ann Cardiol Angéiol* 1986;7:367–371.
16. Cerqueira M, Harp G, Ritchie J. Quantitative gated blood-pool tomographic assessment of regional ejection fraction: definition of normal limits. *J Am Coll Cardiol* 1992;20:934–941.
17. Mertz L, Constantinesco A, Brunot B, Germain P, Ravier S, Roul G. G-SPECT and MRI comparison of end-systolic and end-diastolic left ventricular volumes [Abstract]. *Med Nucl* 1995;19:433.
18. Sheehan F, Stewart D, Dodge H, Mitten S, Bolson E, Brown B. Variability in the measurement of regional left ventricular wall motion from contrast angiograms. *Circulation* 1983;68:550–559.
19. Iskandrian A, Schelbert H. Introduction. *J Nucl Med* 1994;35(suppl):1S–3S.
20. Ross J. Myocardial perfusion-contraction matching: implications for coronary heart disease and hibernation. *Circulation* 1991;83:1076–1083.
21. Eisner R, Schmarkey S, Martin, et al. Defects on SPECT "perfusion" images can occur due to abnormal segmental contraction. *J Nucl Med* 1994;35:638–643.
22. Nicolai E, Cuocolo A, Pace L, et al. Assessment of systolic wall thickening using technetium 99m-methoxyisobutylisonitrile in patients with coronary artery disease: relation to thallium-201 scintigraphy with reinjection. *Eur J Nucl Med* 1995;22:1017–1022.
23. Constantinesco A, Mertz L, Brunot B. Dual-isotope (^{201}Tl and ^{99m}Tc-red blood cells) gated SPECT technique for simultaneous assessment of left ventricular perfusion and motion [Abstract]. *J Nucl Cardiol* 1995;2:S18.